Simulating glories and cloudbows in color

Stanley D. Gedzelman

Glories and cloudbows are simulated in color by use of the Mie scattering theory of light upwelling from small-droplet clouds of finite optical thickness embedded in a Rayleigh scattering atmosphere. Glories are generally more distinct for clouds of droplets of as much as ~10 μm in radius. As droplet radius increases, the glory shrinks and becomes less prominent, whereas the cloudbow becomes more distinct and eventually colorful. Cloudbows typically consist of a broad, almost white band with a slightly orange outer edge and a dark inner band. Multiple light and dark bands that are related to supernumerary rainbows first appear inside the cloudbow as droplet radius increases above ~10 μm and gradually become more prominent when all droplets are the same size. Bright glories with multiple rings and high color purity are simulated when all droplets are the same size and every light beam is scattered just once. Color purity decreases and outer rings fade as the range of droplet sizes widens and when skylight, reflected light from the ground or background, and multiply scattered light from the cloud are included. Consequently, the brightest and most colorful glories and bows are seen when the observer is near a cloud or a rain swath with optical thickness of ~0.25 that consists of uniform-sized drops and when a dark or shaded background lies a short distance behind the cloud.

OCIS codes: 010.1290, 280.1310, 190.4020, 290.4210, 330.1690.

1. Introduction

Glories and cloudbows are luminous phenomena that surround an observer's shadow on a cloud deck or fog bank. Before the age of powered flight, glories were seldom seen but tended to be described in almost ecstatic terms by mountaineers and balloonists.[1–4] Glories are now seen almost routinely from airplanes flying high over cloud decks, yet rarely are they bright and colorful enough to evoke much excitement. In many cases the glories are accompanied by cloudbows so faint, broad, and colorless that they are seen only by a trained eye.[5] There are, however, many reports and photographs of bright cloudbows, usually seen in mist or fog.[6,7]

Glories and cloudbows are produced when sunlight or moonlight is backscattered from clouds of small droplets. Their brightness, color, and angular size depend on the ratio of the particle circumference ($2\pi a$) to the wavelength of light (λ), i.e., the size parameter $x \equiv 2\pi a/\lambda$. Scattering of light by small spherical particles is given by Mie theory, although there are several other approaches and approximations.[8–11] The Mie backscatter peak that corresponds to the glory is pronounced and colorful when the size parameter lies in the approximate range 10–300.[12,13] For particles smaller than ~1 μm in radius the backscatter peak decreases and ultimately disappears. The spacing between glory rings is inversely proportional to the size parameter, so when particles are larger than ~30 μm in radius the rings begin to merge into a diffuse backscatter peak hastened by the finite angular width of the Sun. Thus most aerosol particles do not produce visible glories, but almost all fog and nonprecipitating clouds can. The global average drop radius in water clouds, typically marine stratus, clusters about 10 μm but in localized regions varies from roughly 2 to 20 μm.[14–17] The average droplet radius is smaller in continental clouds because cloud condensation nuclei are more numerous.

As drop size increases, the glory shrinks and fades while the cloudbow becomes more prominent (Fig. 1).[1,17] The Mie scattering peaks that correspond to the cloudbow appear first when x is ~20 or for a droplet radius of ~2 μm. As droplet size increases above ~6 μm the cloudbow takes shape as a broad white band with a dark inner band. As droplet size increases above ~10 μm the inner edge of the cloudbow acquires an orange tone and higher-order light and dark bands appear inside the primary cloudbow—the first hint of the supernumerary rain-

The author is with the Department of Earth and Atmospheric Sciences and the Center for Remote Sensing Science and Technology, City College of New York, New York, New York 10031 (stan@scisun.sci.ccny.cuy.edu).

Received 27 February 2002; revised manuscript received 7 May 2002.

0003-6935/03/030429-07$15.00/0

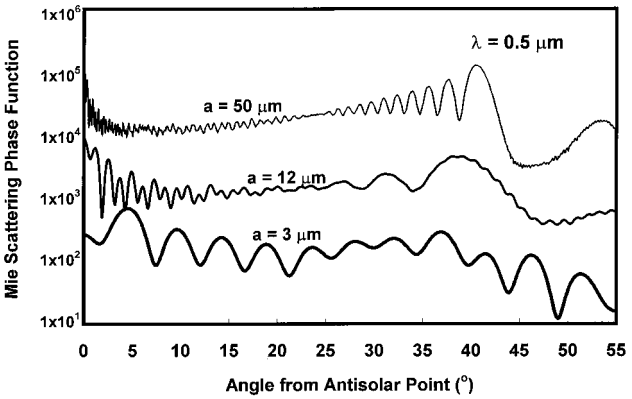

Fig. 1. Mie scattering phase functions for a point Sun for droplet radii 3, 12, and 50 μm at λ = 0.5 μm, showing decreasing angular size of glory and increasing prominence of cloudbow as droplet radius increases.

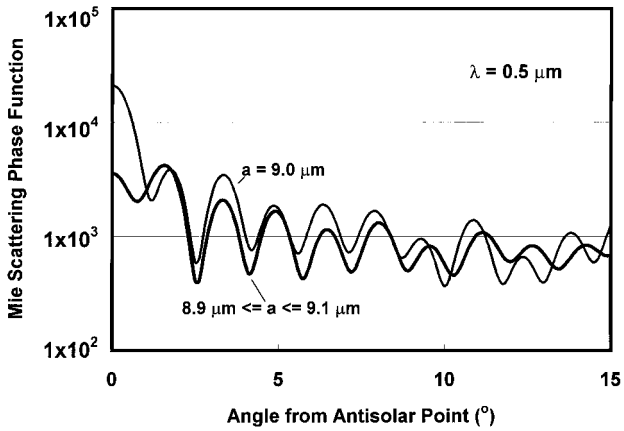

Fig. 2. Comparison of Mie scattering phase functions about the antisolar point at λ = 0.5 μm for a = 9.0 μm and for an average over 21 equally spaced radii from 8.9 and 9.1 μm. Amplitudes of scattering peaks and troughs change rapidly with radius, but angles do not.

bows. Once droplet radius exceeds ~50 μm, well-defined rainbow colors begin to appear.[18] Such large drops occur only in rain clouds and are seldom found near cloud top.

Observed peaks of brightness and color purity of glories and cloudbows rarely approach the maxima given by Mie scattering theory for a single particle. Interference effects seriously reduce peaks of color purity and brightness and may obliterate the outer rings whenever there is a broad drop size distribution, as is the case in most clouds. Under such conditions, the glory is reduced to a bright, inner pale yellow ring and a single red ring. Laven[19] reports that an inner blue ring of glories is seldom distinctly visible even if outer red rings can be seen. The blue ring is easily washed out by interference caused by a drop size distribution because it occurs in a brightness minimum.

Skylight, reflected light from the ground, and multiply scattered light from the cloud vitiate the visual contrast of glories and bows. Thus natural glories and bows must be treated as problems of radiative transfer.[20–25] They stand out best when the observer is located near the cloud when the background is dark and nearby, and when the cloud or rain swath has an optical thickness τ of approximately 0.05–1.[23,24]

Cloud optical thickness plays a primary role in the visual contrast of glories and bows. At small values of τ the glory and the bow are swamped by skylight or reflected light from the background. At large values of τ, multiply scattered light dominates, and the drop size distribution broadens such that glories and bows are again largely swamped. This is why glories and cloudbows are rarely seen on the sunlit sides of towering cumulus and cumulonimbus.

In this paper, glories and cloudbows are simulated in color. Light beams from the finite-sized Sun are subject to Mie scattering by a size distribution of spherical drops in a cloud layer of finite optical thickness, Rayleigh scattering in the clear air surrounding the cloud, and reflection at the ground. Glories and bows produced by the cloud model are compared with those produced by a so-called perfect Mie scattering model in which each sunbeam is scattered once by a cloud droplet and no other sources of scattering are included.

2. Perfect Mie Scattering Model

Perfect scattering models, in which each light beam from the finite-sized Sun strikes a droplet and is scattered only once, have been used to indicate the potential brightness and color purity of halos, rainbows, coronas, and glories even though they provide an unattainable standard of comparison.[26–28] I obtained the perfect scattering model of the glory and the cloudbow used here by taking appropriately weighted averages of Mie scattering phase functions at 0.1° intervals. At each scattering angle, the resulting phase function is weighted by the Mie scattering efficiency for the size parameter, the spectrum of sunlight (here set equal to the Planck blackbody radiation curve for T = 5700 K), and the number concentration of droplets times their geometrical cross section area. Model clouds with as many as five different droplet radii with simple, symmetric drop size distributions (e.g., with relative number concentrations 1, 3, 5, 3, and 1 for droplet radii 3.0, 3.5, 4.0, 4.5, and 5 μm, respectively) are used to approximate the effect of the plethora of theoretical drop size distributions. A total of 61 uniformly spaced wavelengths from 0.4 to 0.7 μm are included in the color analysis. The wavelength resolution is adequate for the most part but causes faint, spurious color bands in regions of brightness minima, particularly for large droplets. These bands disappear when the calculations include 600 wavelengths,[28] but the resulting computation time is prohibitive in a multiple scattering model.

For small droplets, Mie scattering near the antisolar point varies rapidly with droplet size.[24] Figure 2 indicates that these variations do not impair the

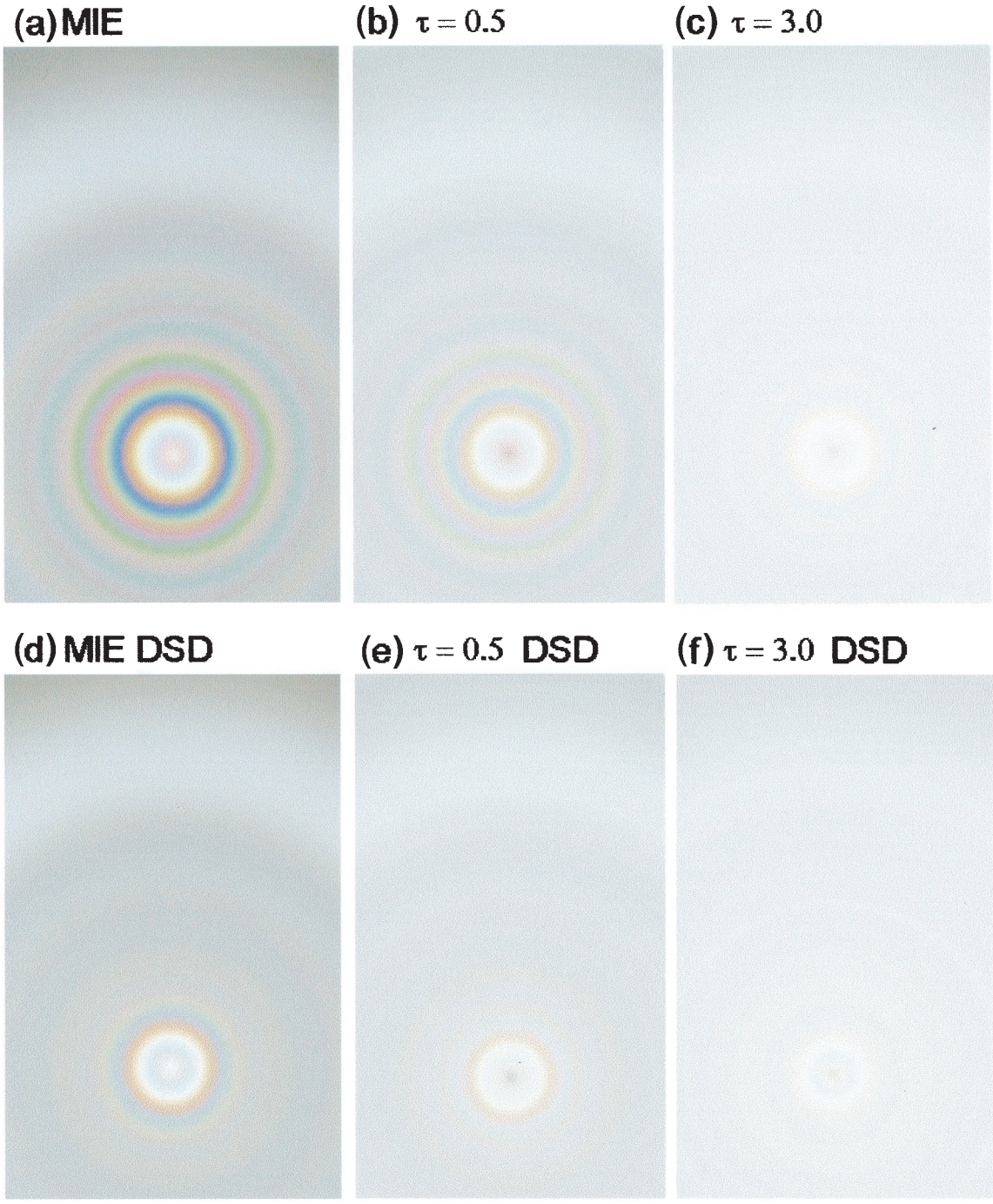

Fig. 3. Smoothed color maps of simulated glories and cloudbows produced by a perfect Mie scattering model (MIE), clouds of optical thickness $\tau = 0.5$ and $\tau = 3.0$, and drop size distributions (DSD) centered at $a = 4$ μm (see text). For cloud simulations the observer stands at cloud edge (800 hPa) with background of albedo 0.03 immediately behind the cloud.

glory because they affect only the magnitude and not the scattering angles of the Mie scattering peaks. To reduce the amplitude of these high-frequency oscillations, I averaged the Mie scattering phase function at each radius and wavelength over 21 closely spaced radii (e.g., from 3.95 to 4.05 μm). This process was independent of considerations of a cloud's drop size distribution.

Clouds of uniform-sized droplets produce the most intense and spectrally pure glories, as Fig. 3 indicates. The color sequence of the glory does not vary much with droplet size, even at small radii. This is one respect in which the glory differs markedly from the corona.[26,29] At the center of the glory is a pastel region of modest brightness. This is surrounded by a bright ring that grades outward from pale blue to pale yellow. Maximum color purity for the glory occurs in the inner red–orange ring, roughly $(20/a)°$

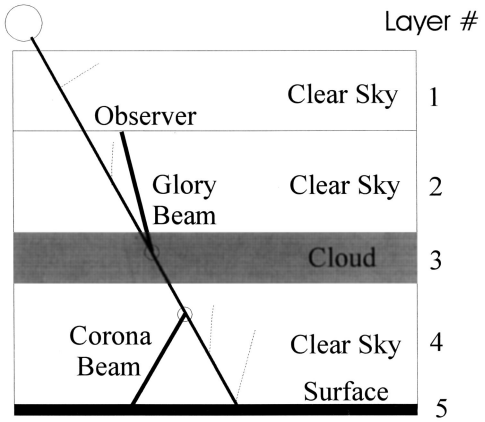

Fig. 4. Five-layer glory model. Light can be scattered multiple times in any layer. All scattered beams that well up to the observer at the top of layer 2 are counted, but only those that are scattered once in the cloud, but nowhere else, contribute to the glory.

from the antisolar point when the radius is given in micrometers. Outside the red ring, color grades from deep blue at a brightness minimum to green to yellow. Four more red–purple rings are distinctly visible for the monodisperse cloud, but, because they decrease in color purity and do not correspond to brightness peaks, they are easily washed out. The sky is dark just inside the cloudbow and tinged orange just outside it.

Even moderately dispersed drop size distributions seriously erode the glory's outer rings. When droplets range from 3 to 5 μm with number concentration (1–3–5–3–1), features out to the second red ring are still distinct, although they become progressively less pronounced away from the antisolar point. All features of the glory beyond the second red ring are faint apparitions at best.

3. Cloud Model

The cloud model, shown in Fig. 4, consists of a five-layer sandwich and is almost identical to the model used to simulate coronas.[29] A geometrically thin cloud in which Mie scattering by drops takes place is embedded in a Rayleigh scattering atmosphere. The clear sky above cloud top at p_{cld} is divided into a layer above the observer at $p = p_{obs}$ and a layer between the observer and the cloud. The ground, located at p_{sfc}, is included as the fifth layer because reflected light adds significant background illumination until clouds become optically thick.

Even though the model consists of horizontal layers, one can apply it to rain swaths or fog banks by adjusting p_{sfc}, p_{obs}, p_{cld}, τ, surface albedo, solar zenith angle, and the Rayleigh scattering coefficient K_{RAY}. For example, multiplying K_{RAY} by the secant of the solar zenith angle will approximate rainbows produced when the Sun is near the horizon. Glories and cloudbows produced in this way take on a red cast.

The model employs a Monte Carlo approach. At each wavelength, roughly 1–2 $\times$ 10^6 light beams are emitted from the finite-sized Sun (assumed to be a Planck radiator at 5700 K) when $\tau > 0.1$, and twice as many when $\tau \leq 0.1$. In each layer a random-number generator determines whether and where a scattering event takes place. Despite the large number of beams and scattering events, which require run times of more than 1 h on a 1-GHz PC when $\tau = 1$, results are still somewhat erratic, as can be seen from Fig 5(b).

At each scattering event, the scattering angle is determined from a random-number generator by use of Rayleigh or Mie angular phase functions. The glory rays are those that reach the observer after being scattered only once in the cloud. Added to this is incoherent light that was multiply scattered within the cloud. In addition, if the observer is located far above cloud top, much light scattered in the intervening clear sky both reduces the glory's intensity and imparts a blue cast that detracts from the cloud's color purity. Light reflected from the ground is assumed to be independent of wavelength and isotropic (Lambertian), even though most Surfaces are colored and have specular reflection peaks. Typical surface albedos range from 3% to 10%.

The model was run for droplet radii of 1.0–100 μm and cloud optical thicknesses) of 0.02–10.0. All figures of the glory in this paper represent azimuthal averages of color dot maps (not shown here) for light scattered about the antisolar point. Averaging was necessary to produce more-reliable results, but it eliminates the natural asymmetry of glories and cloudbows near the horizon.

Chromaticity coordinates (x,y) were calculated as a function of scattering angle by use of equal-energy stimulus coefficients and plotted in the chromaticity diagrams of Fig. 5. Glories produced by a perfect Mie scattering cloud [Figs. 3(a) and 5(a)] had the highest color purity and at least three distinct rings when the cloud consisted of a single droplet size (a = 4.0 μm). Including multiple scattering in a monodisperse cloud of optical depth 0.5 [Figs. 3(b) and 5(b)] reduced the glory's color purity, but outer rings could still be seen. Indeed, outer rings can still be seen at optical depth 3.0 in a monodisperse cloud [Fig. 3(c)]. Broadening the droplet size spectrum in a perfect Mie scattering cloud [Figs. 3(d) and 5(c)] not only reduced color purity but caused the outer rings to disappear.

A heuristic approach was used to match the appearance of observations and photographs of glories and cloudbows to the simulations on the monitor shown in Fig. 3[30] To correct for the monitor's limited color range and excessive apparent color saturation I reduced the distance, r, of each (x, y) point from the tristimulus neutral point ($x = 0.3503$, $y = 0.3616$) to an effective distance $r_{eff} = r^{1.4}$. To compensate for the monitor's nonlinear response to light intensity I seated the RGB values for each point by 255 $\times$ $(I/I_{max})^{0.2}$, where I_{max} is the most intense part of the glory. The exponent used here (0.2) is smaller than the standard gamma correction (0.45) of monitors, it reveals more rings than are visible[19] but yields more

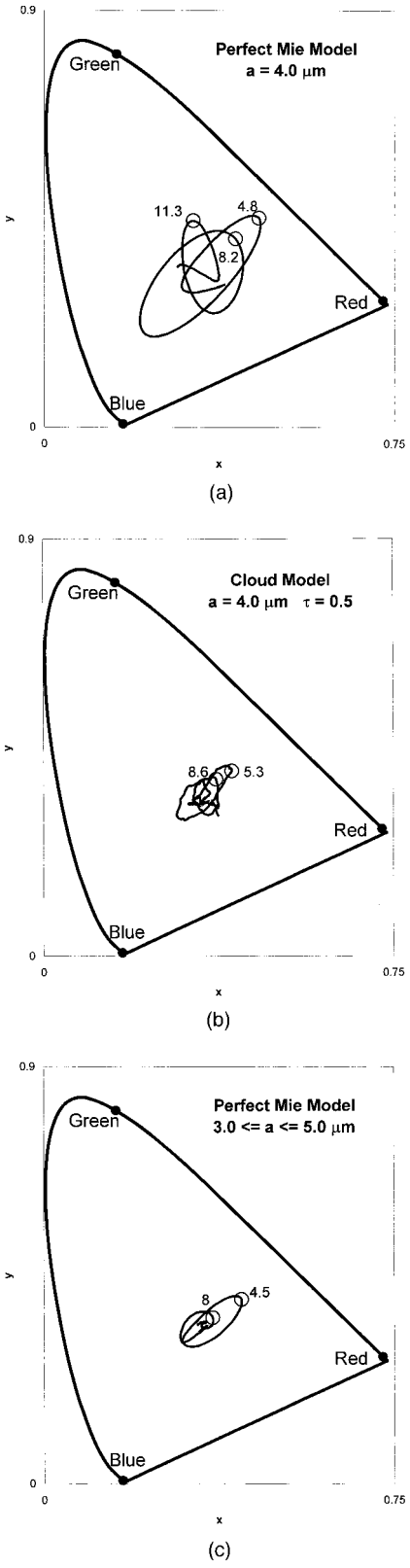

Fig. 5. Chromaticity diagrams from 0° to 15° from the antisolar point for the same situations as in Figs. 3a, 3b, and 3d. (a) Perfect Mie scattering for droplets with 4-μm radii, (b) a cloud of droplets with 4-μm radii and an optical thickness of 0.5, and (c) perfect Mie scattering for a drop size distribution. Red, Green, and Blue work the tristimulus points. Small numbers accompanying open circles represent scattering angle (in degrees) from the antisolar point.

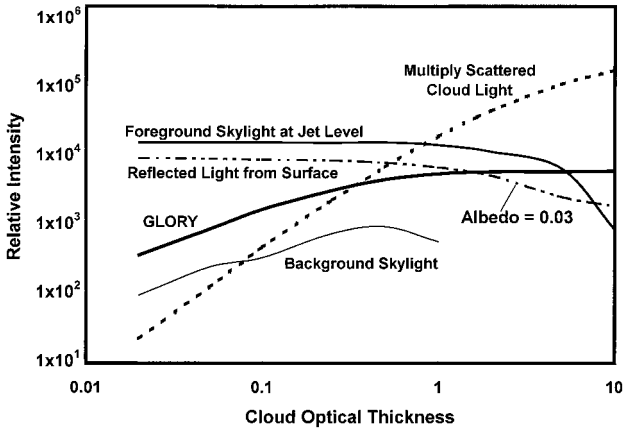

Fig. 6. Brightness of the glory compared to various sources of background illumination as a function of cloud optical thickness. The curve marked Foreground Skylight at Jet Level is for an observer at pressure 300 hPa when cloud-top pressure is 800 hPa and surface pressure is 1013.25 hPa. All other curves are for an observer at cloud edge with the surface immediately behind the cloud.

visually pleasing results.[31] The resulting glory images represent recognizable facsimiles of nature and capture some of the shimmering, translucent quality of the real phenomena after smoothing by the Micrografix Picture Publisher program reduced the abrupt color changes between rings.

4. Discussion

Most glories appear pallid in comparison with glory images that use a perfect Mie scattering model for a single drop size because they are produced by clouds with a range of drop sizes and are seen against backgrounds illuminated by skylight, multiply scattered light from the cloud, and light reflected from the ground. The relative brightness and color purity of glories and cloudbows depend on cloud height and optical thickness, distance of observer to the cloud, surface albedo, atmospheric turbidity, and solar zenith angle as well as on the width of the drop size distribution.

Intensities for the different light sources are shown as a function of cloud optical thickness in Fig. 6 for solar zenith angle 35° and a cloud at a pressure of 800 hPa. The curve marked GLORY is the singly scattered light welling up from the cloud. When the optical thickness is much less than 0.1, the glory is swamped by skylight and reflected light from the surface, even if its albedo is low (i.e., 0.03). Coronas can be seen through clouds with much smaller optical thickness than glories because the Mie forward-scattering peak for small droplets is so pronounced.[29] Diffuse, multiply scattered cloud light is negligible at small cloud optical thickness but dominates at optical thickness greater than ~1. Once optical thickness reaches 10, coronas are no longer visible through the cloud, but glories still shine brightly enough to be seen above the dominant diffuse background lighting.

Skylight is significant at all values of cloud optical

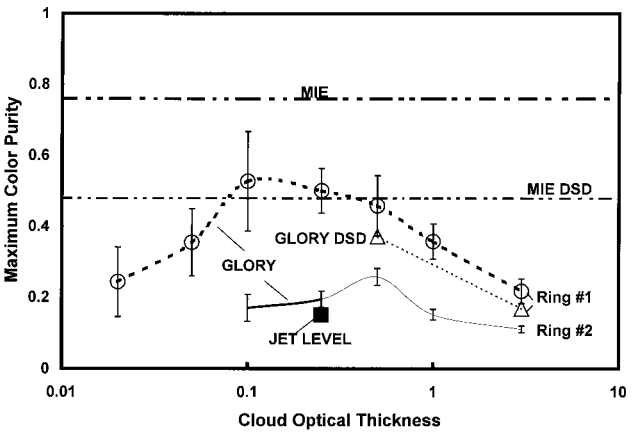

Fig. 7. Maximum color purity of the two innermost red rings Ring #1 and Ring #2, of the simulated glory for the same situations as in Fig. 6 as a function of cloud optical thickness. The maximum color purity of the inner red ring for the perfect Mie scattering model is shown for comparison. DSDs, drop size distributions.

thickness. The model understates the contribution of skylight because includes only Rayleigh scattering. In hazy, turbid atmospheres, skylight can be several times brighter than in a Rayleigh atmosphere and will, as a result, reduce the brightness of the glory beam. In pristine air, the contribution of skylight is relatively small near the cloud, but it increases rapidly as the observer's distance from the cloud increases.

Except for brief moments following take-off and before landing, jet planes fly well above decks of water droplet clouds. Under such conditions, not only does the intervening skylight wash out the glory and the cloudbow but, as distance from the cloud increases, a larger area of cloud is sampled so the effective droplet size spectrum is broader.

For all these reasons, the most dramatic glories and cloudbows occur for an observer in clean air at the edge of a cloud that has a narrow drop size distribution, an optical thickness of roughly 0.25, and a dark surface immediately behind it. But even under these optimal conditions, the glory contributes no more than 25% of the total illumination. Consequently, as Figs. 3, 5, and 7 show, the color purity of glories simulated by the cloud model is much less than for the perfect Mie scattering model.

The glory's outer rings are effectively smudged out by wide drop size spectra, by multiple scattering in optically thick clouds, by skylight (especially in hazy air), and by light reflected from bright surfaces in optically thin clouds. As cloud optical thickness increases beyond 1, multiply scattered light dominates. Even-without skylight or reflected light, only the first two rings appear distinctly once cloud's optical thickness exceeds ~3, and the third ring is a faint visage at best. Thus it makes sense that the first report of a striking glory by Ulloa in the mountains of Peru[4] pointed out that fog was evaporating. The highly restrictive set of conditions required for seeing a bright glory with three or more colorful rings makes the vision all the more breathtaking.

I am thankful to the the participants of the American Meterological Society's and the Optical Society of America's topical meetings on meteorological optics, who have increased my knowledge and love of atmospheric optical phenomena. Several people deserve particular mention here. The Mie scattering calculations are based on a model provided by Jim Lock. I have learned much during discussions and correspondence with Jim Lock, Ray Lee, Chuck Adler, Michael Vollmer, and Ken Sassen. When this manuscript was in the later stages of preparation, I learned of Philip Laven's manuscript,[28] which contains a more-detailed analysis of the perfect Mie scattering solutions for the glory and rainbow. Laven and an anonymous reviewer made incisive comments that improved the quality of the paper. This research was supported by grants from the NASA Tropical Rain Measuring Mission (TRMM) Professional Staff Congress (PSC), City University of New York, and the National Oceanic and Atmospheric Administration Center for Remote Sensing Science and Technology (CREST).

References

1. M. Minnaert, *The Nature of Light and Color in the Open Air* (Dover, New York, 1954), Chap. 10.
2. W. J. Humphreys, *Physics of the Air* (Dover, New York, 1964), Chap. 6.
3. R. A. R. Tricker, *An Introduction to Atmospheric Optics* (American Elsevier, New York, 1970), Chaps. 5 and 7.
4. D. K. Lynch and S. N. Futterman, "Ulloa's observations of the glory, fogbow, and an unidentified phenomenon," Appl. Opt. **30,** 3538–3541 (1991).
5. R. Greenler, *Rainbows, Halos, and Glories* (Cambridge U. Press, Cambridge, 1980), Chap. 1 and 6.
6. D. K. Lynch and W. Livingston, *Color and Light in Nature*, 2nd ed. (Cambridge U. Press, Cambridge, 2001), Chap. 4.
7. "Observer's notebook: the magic of fog," Sky Telescope **87**(5), 110–111 (1994).
8. H. C. van de Hulst, "A theory of the anti-coronae," J. Opt. Soc. Am. **37,** 16–22 (1947).
9. J. A. Adam, "Mathematical physics of rainbows and glories," Phys. Rep. **356,** 229–365 (2001).
10. V. Khare and H. M. Nussenzveig, "Theory of the glory," Phys. Rev. Lett. **38,** 1279–1282 (1977).
11. H. C. Bryant and N. Jarmie, "The glory," Sci. Am. **231,** 60–71 (1974).
12. J. D. Spinhirne and T. Nakajima, "Glory of clouds in the infrared," Appl. Opt. **33,** 4652–4662 (1994).
13. J. A. Lock, "Observability of atmospheric glories and supernumerary rainbows," J. Opt. Soc. Am. A **6,** 1924–1930 (1989).
14. Q. Han, W. B. Rossow, J. Chou, and R. M. Welch, "Global survey of the relationships of cloud albedo and liquid water path with droplet size using ISCCP," J. Clim. **11,** 1516–1528 (1998).
15. M. Kuji, T. Hayasaka, N. Kikuchi, T. J. Nakajima, and M. Tanaka, "The retrieval of effective particle radius and liquid water path of low-level marine clouds from NOAA AVHRR data," J Appl. Meteorol. **39,** 999–1016 (2000).
16. S. Kato, G. G. Mace, E. E. Clothiaux, J. C. Liljegren, and R. T. Austin, "Doppler cloud radar derived drop size distributions in liquid water stratus clouds," J. Atmos. Sci. **58,** 2895–2916 (2001).

17. D. K. Lynch and P. Schwartz, "Rainbows and fogbows," Appl. Opt. **30,** 3415–3420 (1991).
18. R. L. Lee, Jr., "Mie theory, Airy theory, and the natural rainbow," Appl. Opt. **37,** 1506–1519 (1998).
19. P. Laven, European Broadcasting Union, Geneva, Switzerland (personal communication, 2002).
20. S. Twomey, H. Jacobowitz, and H. Howell, "Light scattering by cloud layers," J. Atmos. Sci. **24,** 70–79 (1967).
21. J. E. Hansen and J. B. Pollack, "Near infrared light scattering by terrestrial clouds," J. Atmos. Sci. **27,** 265–281 (1970).
22. S. D. Gedzelman, "Visibility of halos and rainbows," Appl. Opt. **19,** 3068–3074 (1980).
23. S. D. Gedzelman, "Rainbow brightness," Appl. Opt. **21,** 3032–3037 (1982).
24. S. D. Gedzelman, "Simulating rainbows and halos in color," Appl. Opt. **33,** 4607–4613 (1994).
25. E. Tränkle and R. G. Greenler, "Multiple-scattering effects in halo phenomena," J. Opt. Soc. Am. A **4,** 591–599 (1987).
26. J. Lock and L. Yang, "Mie theory model of the corona," Appl. Opt. **30,** 3408–3414 (1991).
27. W. Tape, *Atmospheric Halos*, Vol. 64 of Antarctic Research Series (American Geophysical Union, Washington, D.C., 1994).
28. P. Laven, "Simulation of rainbows, coronas, and glories by use of Mie theory," Appl. Opt. **42,** 436–444 (2003).
29. S. D. Gedzelman and J. A. Lock, "Simulating coronas in color," Appl. Opt. **42,** 497–504 (2003).
30. R. J. Kubesh, "Computer display of chromaticity coordinates with the rainbow as an example," Am. J. Phys. **60,** 919–923 (1992).
31. D. Bruton, "Color science" (1996), http://www.physics.sfasu.edu/astro/color.html.